Cellulose (2009) 16:455–465
DOI 10.1007/s10570-009-9277-1

A technique for production of nanocrystalline cellulose with a narrow size distribution

Wen Bai · James Holbery · Kaichang Li

Received: 14 April 2008 / Accepted: 23 January 2009 / Published online: 11 February 2009

Abstract Nanocrystalline cellulose (NCC) was prepared by sulfuric acid hydrolysis of microcrystalline cellulose. A differential centrifugation technique was studied to obtain NCC whiskers with a narrow size distribution. It was shown that the volume of NCC in different fractions had an inverse relationship with relative centrifugal force (RCF). The length of NCC whiskers was also fractionized by differential RCF. The aspect ratio of NCC in different fractions had a relatively narrow range. This technique provides an easy way of producing NCC whiskers with a narrow size distribution.

Keywords Nanocrystalline cellulose (NCC) · Microcrystalline cellulose (MCC) · Differential centrifugation · Narrow size distribution · Transmission electron microscope (TEM)

Introduction

Cellulose is the most abundant natural polymer and contains both amorphous and crystalline structures. Nanocrystalline cellulose (NCC), also called cellulose nanocrystals, is typically a rigid rod-shaped monocrystalline cellulose domain (whisker) with 1–100 nm in diameter and tens to hundreds of nanometers in length (Ruiz et al. 2000; de Souza Lima and Borsali 2004). NCC has a highly crystalline structure, a very large aspect ratio (around 70), and a high surface area (ca. 150 m^2/g) (Ruiz et al. 2000). Extensive studies have shown that NCC can be used for many applications such as regenerative medicine (Fleming et al. 2001), optical application (Revol et al. 1998), automotive application (Hill 1997; Dahlke et al. 1998), composite materials and so on. NCC has a very high tensile strength, a very high Young's modulus and should be a very good reinforcing filler for various composite materials (Ruiz et al. 2000; Samir et al. 2005; Sakurada et al. 1962). Several studies have shown that NCC serves as a reinforcing filler to dramatically increase the strength of reinforced thermoset and thermoplastic materials (Helbert et al. 1996; Grunert and Winter 2000; Winter and Bhattacharya 2003; Roman and Winter 2006). The geometrical features of NCC are important factors that determine the strength of NCC-reinforced composite materials (Terech et al. 1999; Samir et al. 2004a, b).

Previous studies show that NCC can be produced from acid hydrolysis of various natural cellulose fibers such as cotton, cellulose fibers from lignocellulosic materials, and a marine animal tunicate (Grunert and Winter 2000, 2002; Dong et al. 1998; Edgar and Gray 2002; Heux et al. 2000).

W. Bai · K. Li (✉)
Wood Science & Engineering Department, Oregon State University, Corvallis, OR 97331, USA
e-mail: kaichang.li@oregonstate.edu

J. Holbery
Energy and Environment Directorate, Pacific Northwest National Laboratory, Richland, WA 99352, USA

Microcrystalline cellulose (MCC) from lignocellulosic materials such as wood is abundant, inexpensive and readily available. Therefore, NCC is commonly produced from the hydrolysis of MCC with a strong acid such as sulfuric acid (Bondeson et al. 2006). The acid hydrolysis removes the amorphous cellulose to form highly crystalline cellulose, and also reduces the size of MCC. NCC from acid hydrolysis of MCC typically has a wide range in size. Geometrical characteristics of NCC depend on the hydrolysis conditions such as temperature and time (Dong et al. 1998), and the original source of cellulose fibers: bacterial cellulose (Grunert and Winter 2000, 2002), cotton filter paper (Dong et al. 1998; Edgar and Gray 2002), and tunicates (Heux et al. 2000). The size of NCC from previous studies all has a wide range and little has been published on how to produce NCC with a narrow distribution of size.

In this paper, we have developed a novel technique of differential centrifugation to separate NCC suspensions into different fractions with each fraction having a narrow size distribution.

Experimental methods

Chemicals

MCC (Avicel pH-101, $\sim$50 μm) was purchased from FMC BioPolymer (Philadelphia, PA, USA). Sulfuric acid (95–98 wt%) was purchased from Fisher Scientific (Gibbstown, NJ, USA). All water utilized throughout the experimental procedures was deionized water. Uranyl Acetate and copper grids (200 mesh, covered with carbon film) were purchased from Ted Pella Incorporated (Redding, CA, USA).

Preparation of NCC suspensions

NCC suspension was produced by following a literature procedure (Dong et al. 1998). MCC powder (10.0 g) was hydrolyzed by sulfuric acid (87.5 mL, 64% w/v) for 5 h at 45 °C with continuous stirring. The hydrolysis was quenched by adding a large amount of water (500 mL) to the reaction mixture. The resulting mixture was cooled to room temperature (25 °C) and centrifuged (2,383*g* or 3,500 rpm) for 30 min at room temperature (Labofuge 400, Heraeus, Hanau, Germany). The supernatant was decanted. Water (500 mL) was added to the precipitate and the mixture was then sonicated for 10 min to form a new suspension. This centrifugation/sonication process was repeated three times. The newly generated suspension was filtered with an ultrafiltration membrane (30,000 molecular weight cutoff) using an Amicon Stirred Cell (Millipore Corporation, Bedford, MA, USA) until the pH of the suspension reached a constant value. The resultant NCC suspension (around 0.2 wt%) was stored in a refrigerator at 3.0 °C.

Transmission electron microscopy (TEM) graphs

An NCC suspension was placed on a copper grid (the drop size of the suspension was around 2.5 mm in diameter) and dried at room temperature (25 °C). The sample was stained with uranyl acetate (around 5 wt%) for 3 min (Zimmermann et al. 2006). TEM graphs were acquired with Philips CM-12 at 60 kV (Philips, Eindhoven, The Netherlands).

Fractionation of NCC suspensions using a differential centrifugation technique

NCC suspensions were separated into six fractions using differential angle velocity, i.e., relative centrifugal force (RCF) at a fixed centrifugal time (10 min). A NCC suspension prepared per the previously described hydrolysis technique was centrifuged at an angular velocity of 500 rpm for 10 min. The precipitate from this centrifugation was discarded because the most whiskers of the precipitate had diameters over 100 nm. The suspension from the previous centrifugation at 500 rpm was centrifuged at 1,000 rpm for 10 min. The precipitate from this centrifugation was designated as Fraction #1. The suspension from the previous centrifugation at 1,000 rpm was centrifuged at 1,500 rpm for 10 min, and the resultant precipitate was designated as Fraction #2. The suspension from the previous centrifugation at 1,500 rpm was centrifuged at 2,000 rpm for 10 min, and the resultant precipitate was designated as Fraction #3. The suspension from the previous centrifugation at 2,000 rpm was centrifuged at 2,500 rpm for 10 min, and the resultant precipitate was designated as Fraction #4. The suspension from the previous centrifugation at 2,500 rpm was centrifuged at 3,000 rpm for 10 min,

Table 1 Experimental design of NCC fractions by differential RCF at fixed centrifuge time (10 min)

Fraction no.	ω (rpm)	RCF (g)	Average yield of NCC[a] (%)	Standard deviation	Relative weight percentage[b] (%)
1	1,000	195	6.68	±0.54	31.79
2	1,500	438	2.15	±0.34	10.21
3	2,000	778	3.00	±0.14	14.27
4	2,500	1,216	2.50	±0.42	11.90
5	3,000	1,751	1.46	±0.11	6.94
6	3,500	2,383	5.23	±0.13	24.89

[a] The average yield of NCC whiskers was based on the dry weight of MCC used in the hydrolysis. Data were the means of three replicates

[b] The relative weight percentage was defined as the weight of each fraction divided by the total weight of six fractions

and the resultant precipitate was designated as Fraction #5. The suspension from the previous centrifugation at 3,000 rpm was centrifuged at 3,500 rpm for 10 min, and the resultant precipitate was designated as Fraction #6. This sequential centrifugation process was repeated three times. This fractionation experiment is shown in Table 1.

Determination of the diameter, length, and volume of NCC

It has been shown that NCCs from tunicate have ribbon-like morphology (Elazzouzi-Hafraoui et al. 2008). However, numerous evidences from microscopy and light scattering techniques reveal that cellulose crystals have rodlike shape (De Souza Lima and Borsali 2004). Ribbon-like morphology was not observed for the NCCs in our study. Therefore we assume that the NCCs have cylindrical shape in our calculation of the NCC volumes.

Approximately ten TEM graphs were acquired for each NCC fraction and subsequently used to determine the diameter and length of each NCC crystals. At least 80–100 measurements of the diameter and the length were made for each fraction. Adobe Photoshop CS software was used to aid in the determination of the NCC size. All data were analyzed by a statistical method (frequency distribution analysis) with all data exhibiting moderately skewed distributions. The relationship between the volume of NCC and RCF was determined via linear regression analysis.

The volume of each NCC particle is calculated from the diameter (d) and length (L) of the NCC particle according to the Eq. 1.

$$V = \frac{\pi d^2 L}{4} \tag{1}$$

The volume of a NCC particle for each fraction is reported as the average volume that can be calculated by Eq. 2.

$$\overline{V} = \frac{\sum_{i=1}^{n} V_i}{n} \tag{2}$$

V_i The volume of individual NCC particle, $\overline{V}$ the average volume of NCC in each fraction.

Mechanism of differential centrifugation

Equation 3 shows the relationship between angular velocity and RCF (Boyer 1993).

$$\mathrm{RCF} = 1.118 \times 10^{-6} \omega^2 r \tag{3}$$

where r = radius (mm), ω = angular velocity (rpm).

NCC whiskers were uniformly dispersed in the suspension. The whiskers traveled to the bottom of the tube with a velocity of v when the centrifugal force (F_c), buoyant force (F_b) and frictional force (F_f) were on balance as shown in Fig. 1 (Boyer 1993).

$$F_c = m\omega^2 r \tag{4}$$

$$F_b = m_0 \omega^2 r \tag{5}$$

$$F_f = fv \tag{6}$$

where m = the mass of NCC, ω = angular velocity, r = radius, m_0 = the mass of the displaced water, f = frictional coefficient, v = the velocity of NCC toward the bottom of centrifugation tube.

The force balance on a NCC particle was explained in Eq. 7

$$m\omega^2 r - m_0 \omega^2 r - fv = 0 \tag{7}$$

$$m = \rho_p V \tag{8}$$

$$m_0 = \rho_s V \tag{9}$$

where ρ_s = solvent (water) density, ρ_p = NCC particle density, and V = the volume of a NCC particle.

Equation 10 is derived from Eqs. 7, 8, and 9. To get the relationship between RCF and volume of

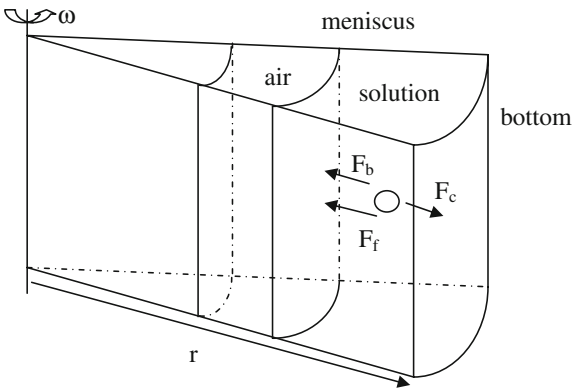

Fig. 1 A schematic of working mechanism of centrifugation. ω Angle velocity, r radius of centrifuge, F_c centrifugal force, F_b buoyant force, F_f frictional force

NCC particle, Eq. 11 is derived from the combination of Eqs. 3 and 10.

$$V = \frac{fv}{\omega^2 r(\rho_p - \rho_s)} \tag{10}$$

$$V = \frac{1.118 \times 10^{-6} fv}{\mathrm{RCF}(\rho_p - \rho_s)} \tag{11}$$

$$V = \frac{Av}{\mathrm{RCF}} \tag{12}$$

$$\log(V) = \log(Av) - \log(\mathrm{RCF}) \tag{13}$$

where $A = \frac{1.118 \times 10^{-6} f}{(\rho_p - \rho_s)}$, A is a constant.

From Eqs. 12 and 13, we can see that the volume (V) is proportional to the velocity v at a fixed RCF. In other words, at a fixed RCF as all centrifugation was done, a bigger NCC would have a higher velocity, i.e., would reach the bottom of a centrifugation tube first. For individual NCC particle, its precipitation speed to the bottom of a centrifuge tube increases along with increase in RCF. For precipitating a small NCC particle, either RCF or centrifugation time has to be increased. At a fixed centrifugation time, NCC fractions with different volume distributions can be obtained through a sequential change in RCF. This is the basic principle behind this work.

Results and discussion

Verification of NCC size by TEM

TEM images of NCC fractions from the angle velocity of 1,000–3,500 rpm revealed that all cellulose whiskers maintained diameters less than 100 nm. A representative TEM image of the cellulose whiskers is shown in Fig. 2. However, the diameters of some cellulose whiskers were larger than 100 nm when the hydrolysis time was less than 5 h. Therefore, the 5 h hydrolysis time was used for generating NCC suspensions in this fractionation study. TEM images were used to determine the sizes of NCC in the fractionation study.

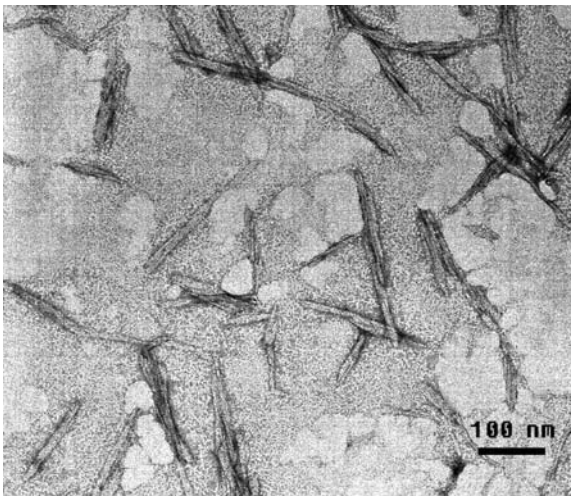

Fig. 2 Transmission electron microscope (*TEM*) image of NCC

Yields of NCC in different fractions

The yield of NCC in each fraction was calculated by the weight of NCC in each fraction divided by the initial weight of MCC. The average yields of NCC from Fraction 1 to Fraction 6 were 6.68, 2.15, 3.00, 2.50, 1.46, and 5.23% (Table 1). The total yield of NCC in six fractions was about 21.02%. The high yields of NCC were in Fraction 1 and Fraction 6 (Table 1). Fraction 1 accounted for 31.79% of all NCCs. The high yield of NCC in Fraction 1 was probably due to a number of large NCC. The relative weight percentages of the Fractions 2–5 were 10.21, 14.27, 11.90, and 6.94%, respectively. The relative weight percentage of NCC in the Fraction 6 was around 24.89%. It also indicated that the number of NCC with small size in Fraction 6 was larger than that of any other fractions.

The relationship between RCF and the volume of NCC in each fraction

The inverse relationship between RCF and the volume (V) of NCC from the Fraction 1 to the Fraction 6 is shown in Fig. 3. The inverse relationship between RCF and volume of NCC whiskers is consistent with the principle of differential centrifugation described in the Method section. R^2 was 0.88 from the simple linear regression analysis, indicating a linear relationship between log(RCF) and log(V). Each data point represented the average volume of NCC whiskers in each fraction (Fig. 3). The standard error of each data point was not shown because all the volume distributions were not normal and moderately skewed. At the same centrifuge time, the larger the centrifuge force, the smaller the precipitated NCC whiskers. However, there was a break point at Fraction 3 (RCF = 778). The average volume of NCC in Fractions 3 was smaller than both Fraction 2 and Fraction 4. The exact reason for this break point is not well understood. The break point at Fraction 3 led to a relatively low value of R^2 (0.88).

The volume distributions of the NCC whiskers from the six fractions are shown in Fig. 4. For the

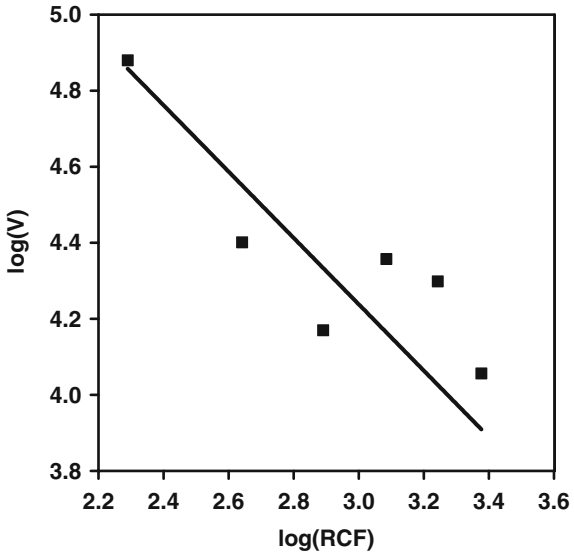

Fig. 3 The inverse relationship between relative centrifugal force (*RCF*) and volume (*V*)* of NCC from Fraction 1 to Fraction 6. *The values of volume at all data points are the average volume of NCC in each fraction. The volume distribution of each fraction is not a normal distribution, so that the standard deviation is not shown in the figure

Fraction 1, about 3.80% of NCC whiskers was in the volume range from 0 to 5×10^3 nm^3 (Fig. 4a). The percentage of NCC whiskers increased to 17.72% in the volume range from 6×10^3 to 10×10^3 nm^3. It decreased to 13.92% in the volume range from 11×10^3 to 15×10^3 nm^3 and further decreased to 10.13% in volume range from 16×10^3 to 20×10^3 nm^3. The right tail (from 66×10^3 to 105×10^3 nm^3) of the volume distribution for the Fraction 1 was 12.66%. For the Fraction 2, 11.58% of NCC whiskers fell within the volume range from 0 to 5×10^3 nm^3. The percentage of NCC increased to 24.21% in the volume range from 6×10^3 to 10×10^3 nm^3. It decreased to 18.95% in the volume range from 11×10^3 to 15×10^3 nm^3 and further decreased to 8.43% in the volume range from 16×10^3 to 20×10^3 nm^3. The right tail (from 66×10^3 to 105×10^3 nm^3) of the volume distribution in the Fraction 2 was 6.32% (Fig. 4a). For the Fraction 3, 28.89% of NCC was in the volume range from 0 to 5×10^3 nm^3. The percentage of NCC was also 28.89% in the volume range from 6×10^3 to 10×10^3 nm^3. It decreased to 13.33% in the volume range from 11×10^3 to 15×10^3 nm^3 and further decreased to 11.11% in volume range from 16×10^3 to 20×10^3 nm^3. The right tail (from 66×10^3 to 105×10^3 nm^3) of the volume distribution in Fraction 3 was only 1.11% (Fig. 4a). For the Fraction 4, 18.12% of NCC was in the volume range from 0 to 5×10^3 nm^3. The percentage decreased to 16.87, 15.62, and 9.38% in volume ranges from 6×10^3 to 10×10^3 nm^3, from 11×10^3 to 15×10^3 nm^3, and from 16×10^3 to 20×10^3 nm^3, respectively. The right tail (from 66×10^3 to 105×10^3 nm^3) of the volume distribution for the Fraction 4 was 4.38% (Fig. 4b). For the Fraction 5, 22.00% of NCC whiskers were in the volume range from 0 to 5×10^3 nm^3. The percentages of NCC in volume ranges from 6×10^3 to 10×10^3 nm^3, from 11×10^3 to 15×10^3 nm^3, and from 16×10^3 to 20×10^3 nm^3 continuously decreased to 30.00, 9.00, and 6.00%, respectively (Fig. 4b). The right tail (from 66×10^3 to 105×10^3 nm^3) of the volume distribution for the Fraction 5 was about 1.00%. For the Fraction 6, about 41.90% of NCC whiskers were in volume range from 0 to 5×10^3 nm^3. The percentages decreased to 23.80, 10.48, and 4.76% in following three volume ranges from 6×10^3 to 10×10^3 nm^3, from 11×10^3 to 15×10^3 nm^3 and

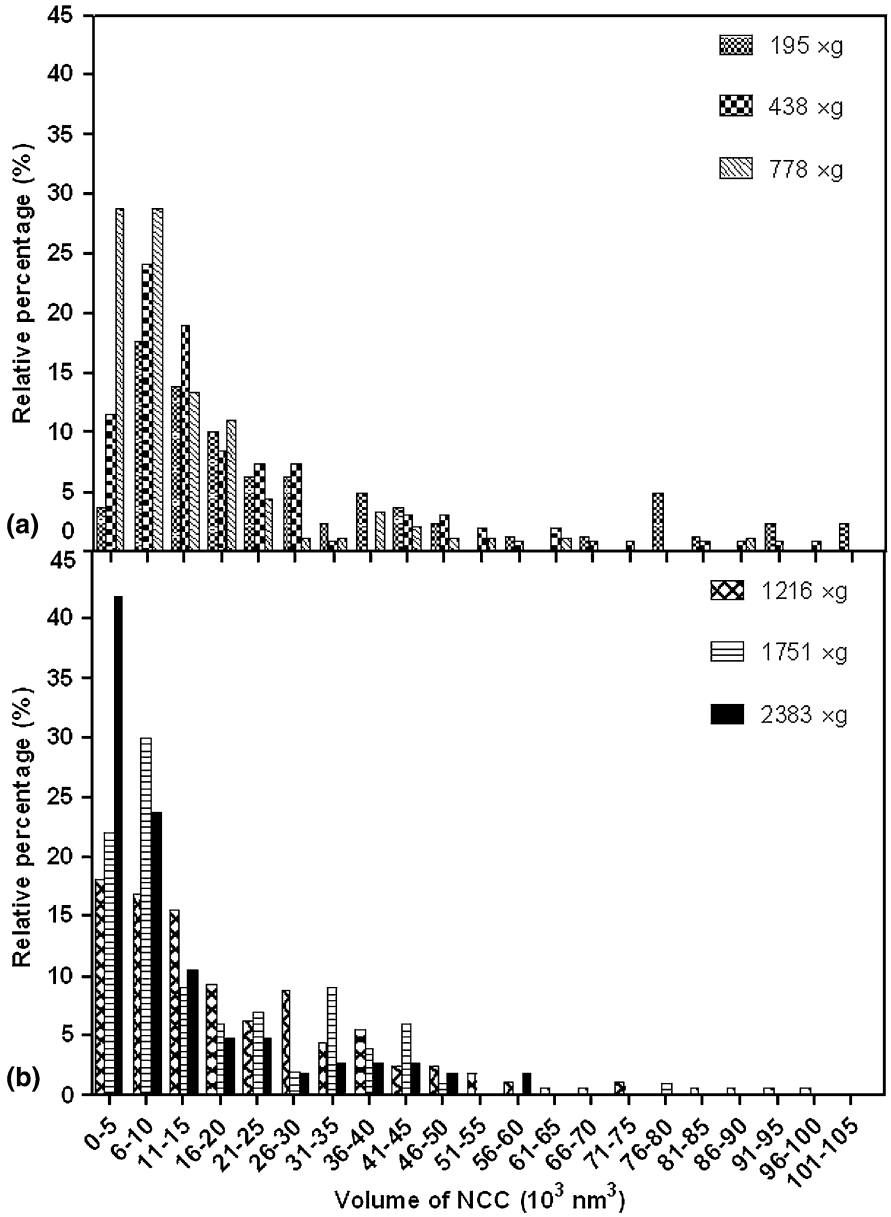

Fig. 4 The volume distribution of NCC after fractionation by differential RCF. *Relative percentage = (Number of NCC whiskers in each bin of one fraction)/(total number of NCC whiskers in one fraction) × 100%. **Legends stand for differential RCF in different fractions

from 16 × 10^3 to 20 × 10^3 nm^3, respectively. There were no NCC whiskers in the right tail (from 66 × 10^3 to 105 × 10^3 nm^3) of the volume distribution for the Fraction 6. The volume of NCC whiskers in each fraction had a distribution and was not a single value because NCC whiskers were uniformly suspended in the water and the travelling distances to the bottom of the centrifuge tube varied. Even though a small centrifuge force was applied to a NCC whisker with a small volume, NCC might precipitate if it was close enough to the bottom of a centrifuge tube. However, there is a general trend in the overall volume distribution. The larger the applied centrifugal force was, the more NCC whiskers with smaller volumes were precipitated.

As seen in Table 2, the majority (80%) of NCC whiskers in each fraction had their volume ranges: the Fraction 1, 0–80 × 10^3 nm^3; the Fraction 2, 0–45 × 10^3 nm^3; the Fraction 3, 0–20 × 10^3 nm^3; the Fraction 4, 0–35 × 10^3 nm^3; the Fraction 5, 0–30 × 10^3 nm^3; and the Fraction 6, 0–20 × 10^3 nm^3, respectively. Compared with the full volume ranges,

Table 2 Comparison between the full volume range and the major volume range of NCC whiskers at differential RCF

Fraction no.	ω (rpm)	RCF (g)	Full volume range[a] (10^3 nm^3)	Major volume range[b] (10^3 nm^3)
1	1,000	195	0–105	0–80
2	1,500	438	0–100	0–45
3	2,000	778	0–90	0–20
4	2,500	1,216	0–100	0–35
5	3,000	1,751	0–80	0–30
6	3,500	2,383	0–60	0–20

[a] The volume range contained all NCC whiskers in one fraction

[b] The major volume range was defined as the narrowest volume range containing 80% of NCC in one fraction

the major (80% of NCC whiskers) volume ranges were relatively narrow. For Fractions 3–5, there was no significant difference in the volume distributions under 95% confidence interval [$p = 0.062$ from one-way ANOVA test for multiple comparison using S-Plus software (Version 8.0, Insightful Corp., Seattle, WA, USA)]. It may be due to the small differences of RCF in these three fractions. Overall, there was ample evidence that the majority of NCC whiskers in each fraction shifted to a small volume and the volume range became narrow as RCF increased. The results from the volume distributions (Fig. 4) were also consistent with the inverse relationship between RCF and the volume of NCC whiskers from Fig. 3.

Length distributions of NCC by differential centrifugation method

The length distributions of NCC whiskers for Fractions 1–6 are shown in Fig. 5. It was obvious that the length distribution became narrow as RCF increased, i.e., the length of NCC whiskers in the Fraction 1 had the broadest distribution and the length of NCC whiskers in the Fraction 6 had the narrowest distribution. For the Fraction 1, no NCC whiskers had their lengths less than 40 nm. Only about 1.26% of NCC whiskers had their lengths ranging from 41 to 60 nm and from 61 to 80 nm, respectively. The percentage increased to 8.86% when the length range increased to from 81 to 100 nm. The major percentages of 16.46, 13.92, and 16.46% corresponded to the length ranges from 101 to 120 nm, 121 to 140 nm, and 141 to 160 nm, respectively. The percentages gradually decreased with the increase in the length of NCC whiskers. The right tail (from 281 to 420 nm) of the length distribution for the Fraction 1 was 15.19%. For the Fraction 2, no NCC whiskers had their lengths less than 20 nm. NCC whiskers with the length range from 21 to 40 nm and from 41 to 60 nm each accounted form about 1.05%. The major percentages of 10.53, 4.21, 22.10, 16.84, 11.58, and 10.52% corresponded to the length ranges from 61 to 80 nm, 81 to 100 nm, 101 to 120 nm, 121 to 140 nm, 141 to 160 nm, and 161 to 180 nm, respectively. The percentage of NCC whiskers began to decrease when the length was higher than 180 nm (Fig. 5a). The right tail (from 281 to 420 nm) of the length distribution for the Fraction 2 was 2.10%. For the Fraction 3, no NCC whiskers had its length range less than 60 nm. About 5.55% of NCC whiskers had its length range from 61 to 80 nm. The major percentages of NCC whiskers were 17.78, 22.22, 16.67, and 11.11% corresponding to the length ranges from 81 to 100 nm, 101 to 120 nm, 121 to 140 nm, and 141 to 160 nm, respectively. The percentage decreased to 5.55% for the length range from 161 to 180 nm. The right tail (from 281 to 420 nm) of the length distribution for the Fraction 3 was only 1.11%. For the Fraction 4, no NCC whisker with its length less than 20 nm could be found. Only 0.83% of NCC whiskers were in the length range from 21 to 40 nm. Another 0.83% of NCC whiskers were in the length range from 41 to 60 nm. The percentage increased to 5.83% in the length range from 61 to 80 nm. The major percentages of NCC whiskers were 10.83, 25.00, 17.92, 10.42, and 15.00% corresponding to the length ranges from 81 to 100 nm, 101 to 120 nm, 121 to 140 nm, 141 to 160 nm, and 161 to 180 nm. The percentage then deceased to 4.58% in the following length range of 181–220 nm. There were no NCC whiskers in the right tail (from 281 to 420 nm) of the length distribution for the Fraction 4 (Fig. 5b). For the Fraction 5, no NCC whiskers with their lengths less than 40 nm could be found. About 6.00% of NCC whiskers were in the length range from 41 to 60 nm. Another 6.00% of NCC whiskers were in the length range from 61 to 80 nm. The majority of NCC whiskers fell into narrow length ranges from 81 to 100 nm (21.00%), 101 to 120 nm (15.00%), and 121 to 140 nm (20.00%). The percentage decreased to 8.00% in the following length range of 141–160 nm. The right tail (from 281 to 420 nm) of the length

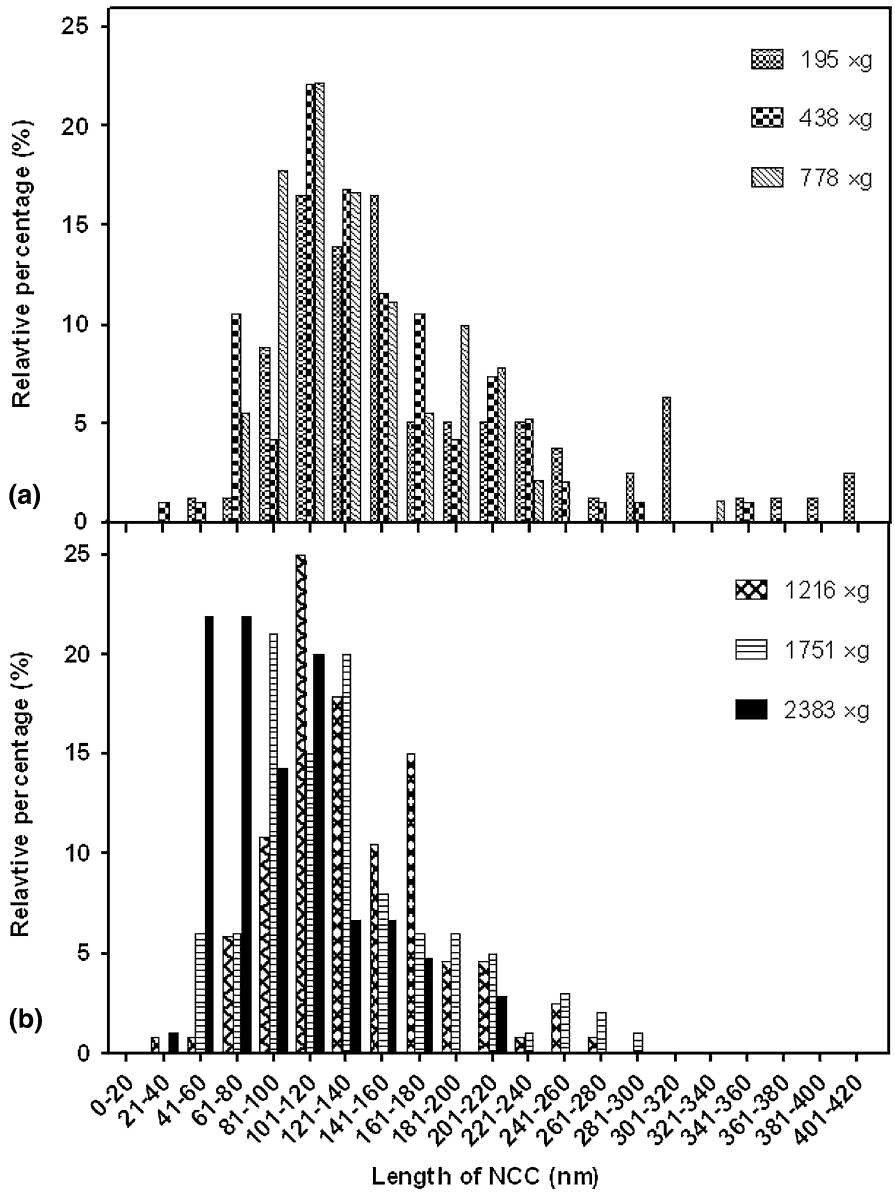

Fig. 5 The length distribution of NCC whiskers after fractionation by differential RCF. *Relative percentage = (Number of NCC whiskers in each bin of one fraction)/(total number of NCC whiskers in one fraction) × 100%. **Legends stand for differential RCF in different fractions

distribution for the Fraction 5 only accounted for about 1.00% of NCC whiskers (Fig. 5b). For the Fraction 6, no NCC whiskers with their lengths less than 20 nm could be found. Only 0.95% of NCC whiskers had its length range from 21 to 40 nm. The major percentages of NCC whiskers were 21.90, 21.90, 14.28 and 20.00%, corresponding to the length ranges from 41 to 60 nm, 61 to 80 nm, 81 to 100 nm, and 101 to 120 nm, respectively. The percentage of NCC whiskers decreased to 6.67% in the following length range of 101–120 nm. No NCC whiskers in the right tail (from 221 to 420 nm) could be found. From the overall length distributions of NCC whiskers, the number of precipitated NCC whiskers with small lengths increased as RCF increased.

Based on the same length range from 41 to 180 nm, the percentages of NCC whiskers from the six fractions were 63% for the Fraction 1, 77% for the Fraction 2, 79% for the Fraction 3, 85% for the Fraction 4, 82% for the Fraction 5, and 96% for the Fraction 6. Table 3 shows the narrowest length ranges containing 90% of NCC whiskers in each

Table 3 Comparison between the full length range and the major length range of NCC whiskers at differential RCF

Fraction no.	ω (rpm)	RCF (g)	Full length range[a] (nm)	Major length range[b] (nm)
1	1,000	195	40–420	81–320
2	1,500	438	30–360	81–220
3	2,000	778	60–340	81–200
4	2,500	1,216	20–280	61–220
5	3,000	1,751	40–280	41–200
6	3,500	2,383	20–220	41–160

[a] The length range contained all NCC whiskers in one fraction

[b] The major length range was defined as the narrowest length range containing 90% of NCC whiskers in one fraction

fraction: 81–320 nm for the Fraction 1, 81–220 nm for the Fraction 2, 81–200 nm for the Fraction 3, 61–200 nm for the Fraction 4, 41–200 nm for the Fraction 5, and 41–160 nm for the Fraction 6. There was a general trend that the length of NCC whiskers decreased when the RCF was increased. The length range also became narrow at the same time. Although the full range of length distribution of NCC in each fraction was broad as indicated in Table 3, the length range containing most NCC whiskers in each fraction was much smaller than the full length range. TEM graphs showed that NCC whiskers were rod-shaped (Fig. 2). The diameter of NCC whiskers was almost ten times less than the length. The variations in the diameter of NCC whiskers were pretty small. This may explain why this differential centrifugation technique can separate NCC whiskers into narrow length ranges.

Aspect ratio distribution of NCC whiskers by differential centrifugation

The aspect ratio of NCC whiskers is defined as L/d, which is length over diameter. The aspect ratio distributions of NCC whiskers for the Fractions 1–6 are shown in Fig. 6. For the Fraction 1, about 82% of NCC whiskers had the aspect ratio between 5 and 16, more specifically, the aspect ratio range of 5–8 (21.52%), 9–12 (39.24%), and 13–16 (21.52%) with the most abundant aspect ratio range being between 9 and 12. For the Fraction 2, about 87% of NCC whiskers had the aspect ratio between 5 and 16, i.e., the aspect ratio range of 5–8 (22.1%), 9–12 (36.84%), and 13–16 (28.42%). The NCC whiskers with the aspect ratio range between 9 and 12 were still more abundant than those with other aspect ratio ranges (Fig. 6). About 65% of NCC whiskers from the Fraction 2 had a very narrow aspect ratio between 9 and 16. For the Fraction 3, about 80% of the NCC whiskers had the aspect ratio between 5 and 20, i.e., the aspect ratio range of 5–8 (12.22%), 9–12 (22.22%), 13–16 (18.89%), and 17–20 (26.67%). The aspect ratio distribution for the Fraction 3 was slightly broader than that for the Fractions 1 and 2. The NCC whiskers with the aspect ratio between 17 and 20 were more abundant than those with other aspect ratio ranges. For the Fraction 4, over 86% of NCC whiskers had the aspect ratio between 5 and 16, i.e., the aspect ratio range of 5–8 (24.38%), 9–12 (40.62%), and 13–16 (21.25%). The NCC whiskers with the aspect ratio of 9–12 were the most abundant. For the Fraction 5, about 78% of NCC whiskers had the aspect ratio between 5 and 16, i.e., 5–8 (26.00%), 9–12 (33.00%), and 13–16 (19.00%). The most abundant NCC whiskers also had the aspect ratio between 9 and 12. For the Fraction 6, about 81% of NCC whiskers had the aspect ratio between 5 and 16, i.e., the aspect ratio range of 5–8 (32.38%), 9–12 (30.48%), and 13–16 (18.10%). In other word, about 63% of NCC whiskers had the aspect ratio between 5 and 12. The aspect ratio distributions for all six fractions were all similar with the most abundant aspect ratio range being between 9 and 12. Except the Fraction 3, more than 78% of NCC whiskers from all other five fractions had their aspect ratio between 5 and 16.

Conclusions

Based on the initial MCC weight, the total yield of NCC whiskers from the sulfuric acid hydrolysis was 21.0%. NCC whiskers obtained from the 5 h hydrolysis had their diameter less than 100 nm. NCC whiskers were successfully fractionized based on their sizes by a new differential centrifugation technique. The volume of NCC whiskers has an inverse relationship with RCF. The experimental data were consistent with the model of differential centrifugation. The majority of NCC whiskers shifted to small sizes and the volume range of NCC also decreased as RCF increased. Furthermore,

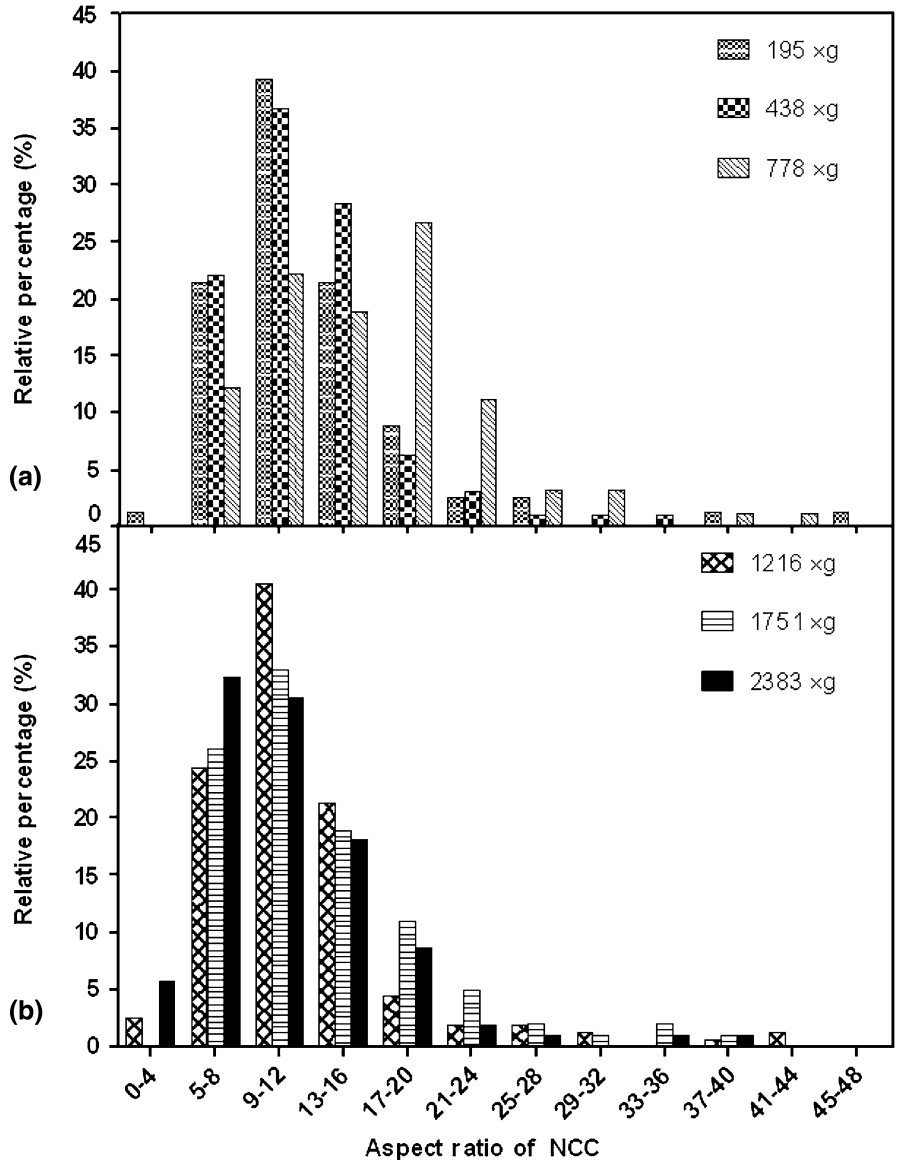

Fig. 6 The aspect ratio distribution of NCC whiskers after fractionation by differential RCF. *Relative percentage = (Number of NCC whiskers in each bin of one fraction)/(total number of NCC in one fraction) × 100%. **Legends stand for differential RCF in different fractions

the length of NCC whiskers also decreased and the length range containing 90% of NCC whiskers became narrow as RCF increased. The aspect ratio distributions of NCC whiskers were in a relatively narrow range. This differential centrifugation technique will allow us to prepare NCC whiskers with a narrow size distribution for various scientific studies and applications.

Acknowledgments Financial support for this research was provided by Schill + Seilacher "Struktol" AG, Hamburg, Germany.

References

Bondeson D, Mathew A, Oksman K (2006) Optimization of the isolation of nanocrystals from microcrystalline cellulose by acid hydrolysis. Cellulose 13(2):171–180

Boyer RF (1993) Modern experimental biochemistry. The Benjamin/Cummings Publishing Company, Inc., Redwood City, p 191

Dahlke B, Larbig H, Scherzer HD, Poltrock R (1998) Natural fiber reinforced foams based on renewable resources for automotive interior applications. J Cell Plast 34:361–379

De Souza Lima MM, Borsali R (2004) Rodlike cellulose microcrystals: structure, properties, and applications. Macromol Rapid Commun 25(7):771–787

Dong XM, Revol J-F, Gray DG (1998) Effect of microcrystallite preparation conditions on the formation of colloid crystals of cellulose. Cellulose 5(1):19–32

Edgar CD, Gray DG (2002) Influence of dextran on the phase behavior of suspensions of cellulose nanocrystals. Macromolecules 35(19):7400–7406

Elazzouzi-Hafraoui S, Nishiyama Y, Putaux J-L, Heux L, Dubreuil F, Rochas C (2008) The shape and size distribution of crystalline nanoparticles prepared by acid hydrolysis of native cellulose. Biomacromolecules 9(1):57–65

Fleming K, Gray DG, Matthews S (2001) Cellulose crystallites. Chem Eur J 7(9):1831–1835

Grunert M, Winter WT (2000) Progress in the development of cellulose reinforced nanocomposites. Polym Mater Sci Eng 82:232

Grunert M, Winter WT (2002) Nanocomposites of cellulose acetate butyrate reinforced with cellulose nanocrystals. J Polym Environ 10(1/2):27–30

Helbert W, Cavaille JY, Dufresne A (1996) Thermoplastic nanocomposites filled with wheat straw cellulose whiskers. Part I: processing and mechanical behavior. Polym Compos 17(4):604–611

Heux L, Chauve G, Bonini C (2000) Nonflocculating and chiral-nematic self-ordering of cellulose microcrystals suspensions in nonpolar solvents. Langmuir 16(21):8210–8212

Hill S (1997) Cars that grow on trees. New Sci Febr 153:36–39

Revol JF, Godbout L, Gray DG (1998) Solid self-assembled films of cellulose with chiral nematic order and optically variable properties. J Pulp Pap Sci 24(5):146–149

Roman M, Winter WT (2006) Cellulose nanocrystals for thermoplastic reinforcement: effect of filler surface chemistry on composite properties. ACS Symposium Series 938, Washington, DC, pp 99–113

Ruiz MM et al (2000) Processing and characterization of new thermoset nanocomposites based on cellulose whiskers. Compos Interfaces 7(2):117–131

Sakurada I, Nukushina Y, Ito T (1962) Experimental determination of the elastic modulus of crystalline regions in oriented polymers. J Polym Sci 57:651–660

Samir MASA, Alloin F, Sanchez J-Y, Dufresne A (2004a) Cross-linked nanocomposite polymer electrolytes reinforced with cellulose whiskers. Macromolecules 37:4839–4844

Samir MASA, Alloin F, Sanchez J-Y, El Kissi N, Dufresne A (2004b) Preparation of cellulose whiskers reinforced nanocomposites from an organic medium suspension. Macromolecules 37:1386–1393

Samir MASA, Alloin F, Dufresne A (2005) Review of recent research into cellulosic whiskers, their properties and their application in nanocomposite field. Biomacromolecules 6:612–626

Terech P, Chazeau L, Cavaille JY (1999) A small-angle scattering study of cellulose whiskers in aqueous suspensions. Macromolecules 32:1872–1875

Winter WT, Bhattacharya D (2003) Ecocomposites: cellulose nanocrystal-filled biodegradable polymers. Abstracts of Papers, 225th ACS National Meeting, New Orleans, March 23–27, 2003: CELL-101

Zimmermann T, Pöhler E, Geiger T, Schleuniger J, Schwarller P, Richter K (2006) Cellulose fibrils: isolation, characterization, and capability for technical applications. ACS symposium series 938. American Chemical Society, Washington, DC, pp 33–47